Applied Catalysis B: Environmental 165 (2015) 360–368

Contents lists available at ScienceDirect

Applied Catalysis B: Environmental

journal homepage: www.elsevier.com/locate/apcatb

Preparation and characterization of a novel KOH activated graphite felt cathode for the electro-Fenton process

Yi Wang[a,*,1], Yuhui Liu[a], Kun Wang[b], Shuqin Song[b], Panagiotis Tsiakaras[c,*], Hong Liu[a,d,*,2]

[a] School of Chemistry and Chemical Engineering, The Key Lab of Low-carbon Chemistry & Energy Conservation of Guangdong Province, Sun Yat-sen University, Guangzhou 510275, China
[b] State Key Laboratory of Optoelectronic Materials and Technologies/The Key Lab of Low-carbon Chemistry & Energy Conservation of Guangdong Province, School of Physics and Engineering, Sun Yat-sen University, Guangzhou, China
[c] Department of Mechanical Engineering, School of Engineering, University of Thessaly, Pedion Areos, 38334 Volos, Greece
[d] Chongqing Institute of Green and Intelligent Technology, Chinese Academy of Sciences, Chongqing, 401122, China

ARTICLE INFO

Article history:
Received 30 July 2014
Received in revised form
25 September 2014
Accepted 30 September 2014
Available online 8 October 2014

Keywords:
KOH activation
Graphite felt
Electro-Fenton
H_2O_2 accumulation
DMP degradation

ABSTRACT

In the present investigation, *graphite felt* (GF) activated by KOH at high temperature is adopted as the electro-Fenton cathode for degrading organic pollutants contained in the wastewater. *Scanning electron microscopy* (SEM), *X-ray photoelectron spectroscopy* (XPS) and *contact angle* results show that through KOH activation the *raw graphite felt* (RGF) could be provided with: (i) higher surface area, (ii) more oxygen-containing functional groups, and (iii) more hydrophilicity. Experimental results show that H_2O_2 accumulation concentration reaches the maximal value at −0.7 V of applied cathode potential and the apparent rate constant for *dimethyl phthalate* (DMP) degradation at the AGF-900 (optimized activation conditions: at 900 °C for 1 h) is 0.198 min^{-1}, much higher than that (0.020 min^{-1}) obtained at the RGF (~900% of enhancement). In the meanwhile, AGF-900 possesses good stability without significant performance decay even after 20 reaction cycles and desirable universality for degrading other organic contaminants. Moreover, the comparison with other commonly used materials confirms the effectiveness of AGF-900 as the electro-Fenton cathode. From the obtained results it is shown that KOH activation at high temperature is a desirable way to decorate graphite felt with more functional groups and then make it more applicable as the electro-Fenton cathode to remove organic pollutants in wastewater.

1. Introduction

Advanced oxidation processes (AOPs) [1–7] have been reported as very effective remediation technologies in wastewater treatment. This is due to the action of a highly reactive and non-selective oxidant, hydroxyl radicals (•OH), which can rapidly destroy persistent organic pollutants. Among AOPs, *electro-Fenton* (EF) technology has aroused wide concerns in recent years for effective organic destruction from wastewater. The reaction mechanism of EF technology is very complicated but its main reactions involved can be described as follows [8–11]:

$$O_2 + 2H^+ + 2e^- \rightarrow H_2O_2 \quad (1)$$

$$H_2O_2 + Fe^{2+} + H^+ \rightarrow Fe^{3+} + {}^{\bullet}OH + H_2O \quad (2)$$

$$Fe^{3+} + e^- \rightarrow Fe^{2+} \quad (3)$$

A distinct advantage of EF technology is the *in-situ* electrochemical production of H_2O_2 and the regeneration of Fe^{2+} by the simultaneous reduction of oxygen and Fe^{3+} at the cathode. This can address the problems caused by the traditional Fenton processes, such as the storage and shipment of concentrated H_2O_2 and the generation of Fe^{2+} sludge. From the above reactions, obviously, H_2O_2 generation, via the *oxygen reduction reaction* (ORR) [12,13] (Reaction (1)), plays an important role in the EF technology. As known, the electrocatalytic mechanism and kinetics is heavily dependent on the electrode materials [14]. Accordingly, the efficiency of H_2O_2 generation is directly related to the types and

* Corresponding authors. Tel.: +30 24210 74065; fax: +30 24210 74050.
E-mail addresses: wangyi76@mail.sysu.edu.cn (Y. Wang), tsiak@uth.gr (P. Tsiakaras), liuhong@cigit.ac.cn (H. Liu).
[1] Tel.: +86 20 84110930; fax: +86 20 84110927.
[2] Tel: +86 23 63063783; fax: +86 23 841133654.

http://dx.doi.org/10.1016/j.apcatb.2014.09.074
0926-3373/

properties of the cathode materials for ORR [15]. Thus, to improve the ORR activity of cathode materials to *in-situ* electrochemically generate H_2O_2 is the key step in the EF technology.

Carbonaceous materials [11] have been widely investigated as the cathode in the EF process due to their desirable H_2O_2 generation with the following advantages such as no toxicity, low-cost, good stability, conductivity, low catalytic activity for H_2O_2 decomposition and so on. Nowadays, many carbonaceous materials have been investigated as the EF cathode, such as graphite [16], carbon felt [17–19], graphite felt [20–22], carbon sponge [23], activated carbon fiber [24–26], carbon-PTFE air-diffusion electrode [27–33]. Among them, *graphite felt* (GF) is a promising commercialization cathode material, due to their advantages of large three dimensional active surfaces, chemical resistance, mechanical integrity and easiness to be manufactured. The ORR at the EF cathode is a complicated dynamic process, and its corresponding reaction activity is quite sensitive to the surface properties of cathode materials. Various surface modification methods for carbonaceous material cathodes have been investigated in order to improve the efficiency for ORR electrocatalysis and EF process. As reported, the electrocatalytic activity of GF cathode for generating H_2O_2 through ORR could be significantly enhanced through the surface modification processes [34,35].

As known, KOH activation method is an effective route to change the surface chemistry and structure for *multiwall carbon nanotubes* (MWCNTs), and the method has been used to improve the performance of the electrocatalysts for fuel cells [36,37]. However, up to now, there is almost no investigation about the effects of KOH activated graphite felts for efficient EF cathode. In the KOH activation method, no toxic chemical is involved, and thus it is easy for large-scale production. Consequently, it could be a good alternative and an important approach to improve the cathode efficiency in EF technology.

In the present investigation, KOH activation method was firstly used to modify GF in order to improve the *in-situ* generation of H_2O_2 at GF cathode for EF system. Both surface chemistry and structure were studied, and the electrocatalytic activity for ORR was investigated. Moreover, *dimethyl phthalate* (DMP) was chosen as the main model organic pollutant to assess the performance of the activated GF as EF cathode, because it has been listed as one of the priority pollutants in many countries, and has been used in rapid performance assessment of some AOPs including EF reactions [38–42].

2. Experimental

2.1. Activation of GF

All used chemicals were of analytical grade. The commercial GF (Hunan Jiuhua Carbon High-Tech Co. Ltd., China) was firstly degreased with acetone in an ultrasonic bath for 15 min and then washed with deionized water for several times to remove the residual acetone. After immersion in 1.0 mol L^{-1} NaOH aqueous solution under mechanical stirring for 3 h to make GF more hydrophilic, it was washed with deionized water and then immersed in 6.0 mol L^{-1} KOH aqueous solution under mechanical stirring and heating until KOH crystals were separated out. After that, GF was mixed with KOH crystals and heated in a tube furnace at different temperatures (700, 800, 900, and 1000 °C) for 1 h or at 900 °C for different time (15, 30, 60, and 90 min). The temperature was increased to the objective point at a heating rate of 4 °C min^{-1} from room temperature. In order to avoid the oxidation of GF, N_2 was adopted as the protecting gas during heating treatment of RGF. Then, the treated GF was washed with 1.0 mol L^{-1} HCl aqueous solution and deionized water for several times in sequences to remove the residual KOH till the solution was neutral. Finally, the sample was dried at 85 °C in a vacuum oven for 12 h. For a clear description, the KOH activated samples were denoted as AGF-700, AGF-800, AGF-900, AGF-1000 (treated at different temperatures for 1 h) and AGF-15, AGF-30, AGF-60, and AGF-90 (treated for different time at 900 °C–AGF stands for *activated graphite felt*), respectively.

2.2. Characterization of GF

The surface morphology of the as-prepared products was obtained by *scanning electron microscopy* (SEM) (LEO-1530VP, Germany). *X-ray photoelectron spectroscopy* (XPS) measurements were performed on a ESCALAB 250 spectrometer equipped with XR6 monochromated X-ray source. The contact angle of the water on the surface of samples was performed using a drop shape analysis system (Krüss, DSA100).

2.3. H_2O_2 accumulation and dimethyl phthalate (DMP) degradation

The H_2O_2 generation and DMP degradation experiments were carried out in an undivided cylindrical glass cell of internal diameter equal to 65.0 mm on a Metrohm Autolab PGSTAT302 N instrument. AGF (2.0 cm × 2.0 cm) was used as the cathode (working electrode), a Pt foil (2.0 cm × 1.0 cm) and a *saturated calomel electrode* (SCE) were used as the anode (counter electrode) and the reference electrode, respectively. O_2 was bubbled by a glass tube into the solution at a flow rate of 600 mL min^{-1} close to the cathode to make the solution saturated with O_2 for H_2O_2 generation. In the experiments of H_2O_2 generation, a 0.1 mol L^{-1} Na_2SO_4 aqueous solution with the initial pH value of 3.0 was used as the electrolyte. In the DMP degradation experiments, Fe^{2+} with different concentrations and DMP with an initial concentration of 50.0 mg L^{-1} were added into the above electrolyte. Without specification, the potentials applied in the present investigation were referred to the SCE.

2.4. Analysis

Linear sweeping voltammetry (LSV) was adopted to investigate and identify the potential for ORR under specific conditions. H_2O_2 concentration was determined by the aid of the potassium titaniumoxalate method using a UV–VIS spectrophotometer (TU1810, Universal Analysis, Beijing, China) at its maximum absorption wavelength of 405 nm. The DMP concentration was measured by *high performance liquid chromatography* (HPLC) (Techcomp, LC 2130, Shanghai, China) equipped with a reverse phase column (Waters, XT erra MS C-18, 5 μm) and a UV detector. The mobile phase was a mixed solution of 50% acetonitrile and 50% water (V/V) at room temperature, with a flow rate of 1.0 mL min^{-1}. The column pressure was 10.6 MPa and the detection wavelength was set at 276 nm. The total organic carbon (TOC) concentration was determined by a TOC/TN analyzer (MultiN/C 3100, Analytikjena, Germany) using the standard non-purgeable organic carbon (NPOC) method.

3. Results and discussion

3.1. LSV analysis

As known, for a determined material, a proper cathode potential is quite important to guarantee the effective H_2O_2 generation via ORR. To find a suitable range of applied cathode potential for H_2O_2 generation at AGF, LSV tests were conducted at AGF-900 in the presence of saturated N_2 or O_2 at a scan rate of 30 mV s^{-1} and the results are shown in Fig. 1. In the case of saturated N_2, the only reaction of H_2 evolution exists, which starts from −0.8 V. However, in the case of saturated O_2, ORR starts from 0 V and the corresponding

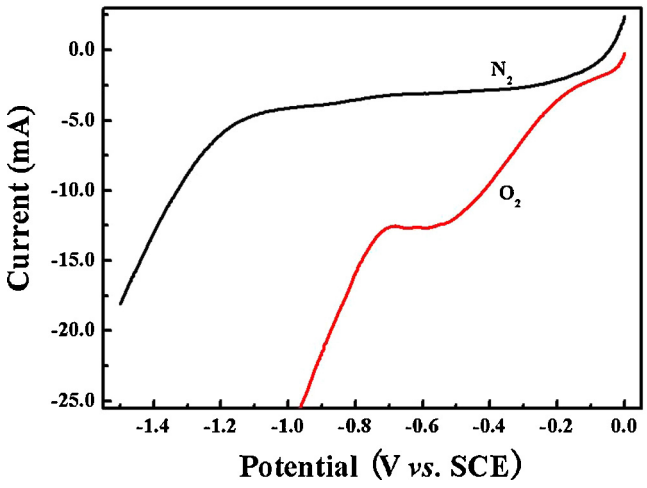

Fig. 1. The linear sweeping voltammetric curves at AGF-900 cathode in 0.1 mol L^{-1} Na_2SO_4 solution (pH = 3.0) in the presence of saturated N_2 or O_2. Potential sweeping rate: 30 mV s^{-1}.

current increases as the potential increases until it reaches a small plateau in the range of about −0.6 V and −0.7 V. After that, the current increases rapidly due to probably both reduction of H_2O_2 to H_2O and the H_2 evolution reaction. Therefore, one can easily infer that the suitable potential range for H_2O_2 generation via ORR at AGF cathode is from −0.6 V to −0.7 V.

3.2. Optimization of KOH activation parameters for GF

In order to obtain the optimal KOH activation parameters for GF, the performance of DMP degradation was adopted as the comparison basis. Their DMP degradation percentage and the corresponding apparent rate constant (k), based on pseudo first-order reaction [43], at RGF and AGF treated at different temperatures for 1 h (700, 800, and 900 °C) and different time (15, 30, and 60 min) at 900 °C, are given in Fig. 2. The KOH activation can greatly increase the DMP degradation performance of RGF and the activation parameters obviously affect the DMP degradation at GF cathode. In 1 h, at RGF, 60% of initial DMP was degraded, with an apparent rate of $k = 0.020\ min^{-1}$. After KOH activation at different temperatures and different time, the initial DMP was almost completely degraded and their corresponding k was significantly enhanced. More precisely, at the sample activated at 900 °C for 60 min (AGF-900 or AGF-60), the k value reached 0.198 min^{-1}, enhanced by almost 9 times with respect to that obtained at RGF. The above significantly improved performance of DMP degradation could be attributed to the increased specific surface area and the decorated oxygen-containing functional groups through KOH activation, which will be discussed below.

In Fig. 3, a comparison of the DMP degradation performances at different GF cathodes is presented. The best DMP performance was obtained at AGF-900 (AGF-60) in the point of view of both DMP degradation percentage and apparent rate constant. Besides, here it is necessary to point out that GF disappeared after its treatment at 1000 °C for 1 h or 900 °C for 1.5 h, which is probably due to the complete reaction between RGF and KOH. Based on the DMP

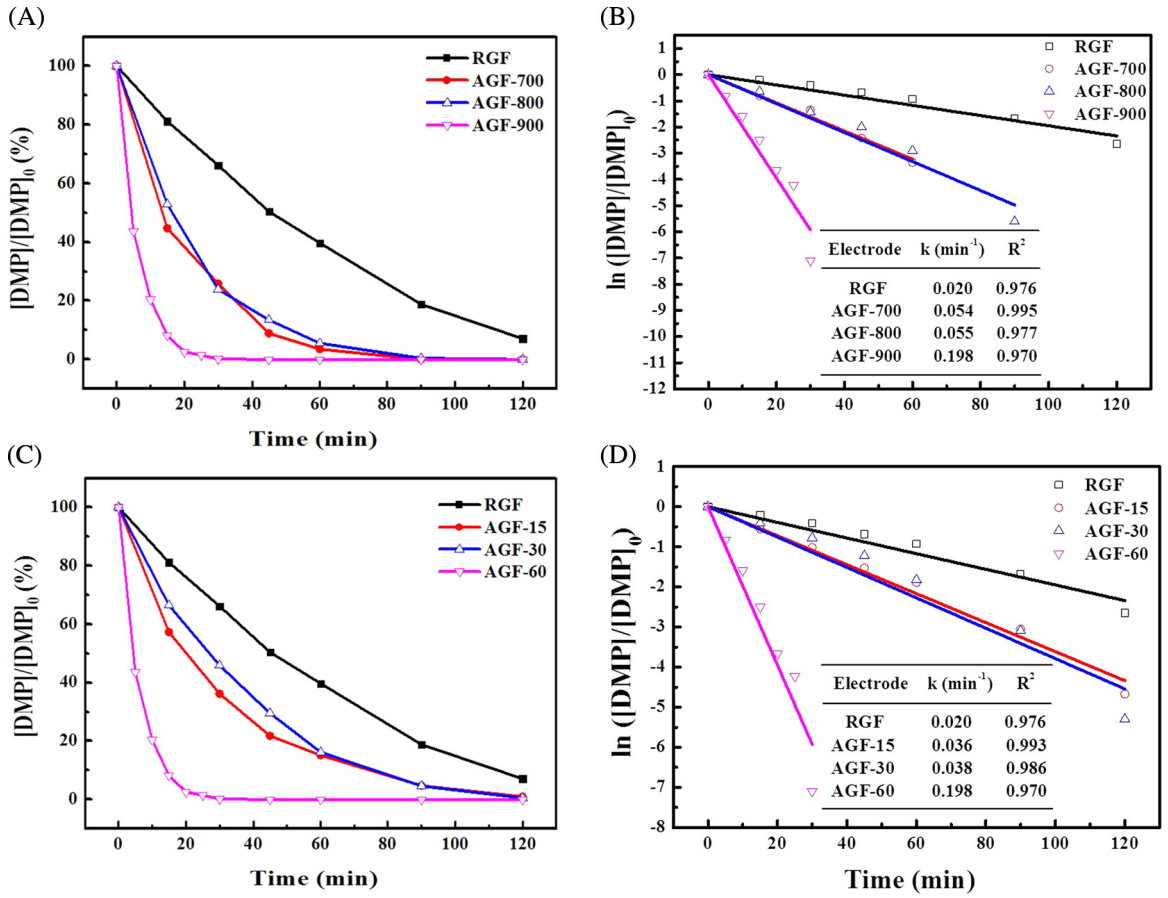

Fig. 2. DMP degradation efficiency and kinetics at RGF and AGF by KOH activation at different temperatures for 1 h (A, B) and different time at 900 °C (C, D). Initial DMP concentration: 50.0 mg L^{-1}, initial pH = 3.0, $[Fe^{2+}] = 0.5$ mmol L^{-1}, applied cathode potential: −0.7 V.

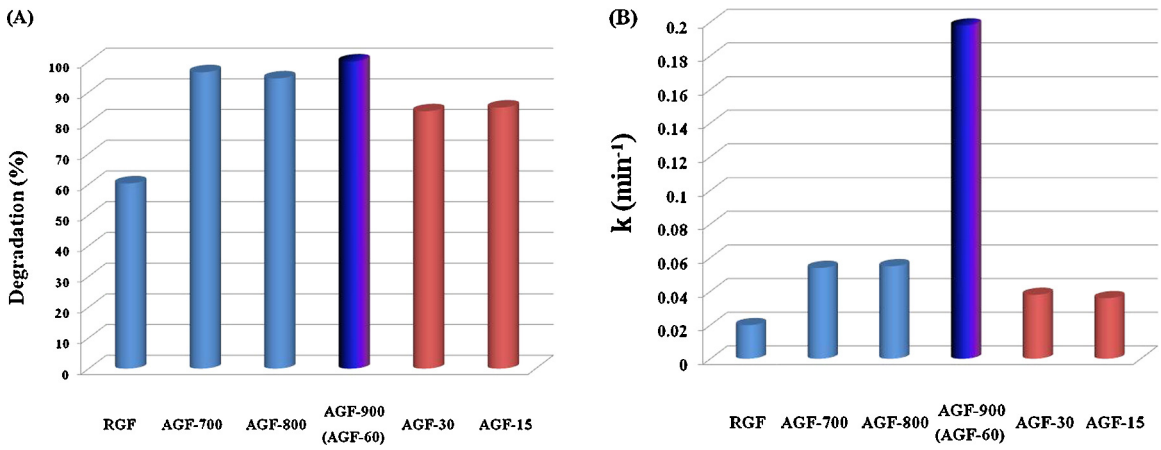

Fig. 3. Comparative results of DMP degradation percentage (A) and their apparent rate constant (B) at RGF and AGF by KOH activation at different temperature values for 1 h and different time values at 900 °C. Initial DMP concentration: 50.0 mg L^{-1}, initial pH = 3.0, [Fe^{2+}] = 0.5 mmol L^{-1}, applied cathode potential: -0.7 V.

degradation performance and the above experimental phenomena, the optimal KOH activation parameters for RGF were at 900 °C for 1 h. So, AGF-900 was adopted for the further investigation including: (i) the physico-chemical characterization by SEM, XPS and contact angle, (ii) the H_2O_2 accumulation, and (iii) the DMP degradation performance, with AGF-900 as the EF cathode.

3.3. Physico-chemical properties of AGF-900

3.3.1. SEM analysis

As clearly shown in Fig. 4A, the surface of RGF is relatively smooth but with some particles, which might be introduced during its production process. While in the case of AGF-900 (Fig. 4B), after KOH activation, these particles are obviously cleaned up. Moreover, the surface becomes relatively rough and there are many grooves, which could be generated from the reaction between C and KOH at high temperatures, through reactions (4) and (5) [37]. These increased roughness and existed grooves will be helpful to increase the specific surface area of the electrode to a great extent and thus increase the active surface area, and in this way promoting the ORR.

$$4KOH + C \rightarrow 4K + CO_2 + H_2O \quad (4)$$

$$6KOH + C \rightarrow 2K + 3H_2 + 2K_2CO_3 \quad (5)$$

3.3.2. XPS analysis

To further understand the surface states of GF after KOH activation, XPS is adopted to analyze their electronic properties and chemical states. Fig. 5 shows the XPS wide scan spectra in the binding energy range of 0–1100 eV for RGF and AGF-900. As it can be distinguished, the peaks for carbon and oxygen are around 284 and 532 eV, respectively. The peak area ratio of O1s to C1s (O/C ratio) is increased from 0.14 to 0.17 for RGF and AGF-900, respectively, indicating that the number of oxygen-containing functional groups are increased after KOH activation.

Peak fitting of C1s and O1s were carried out and the results are shown in Fig. 6. Obviously, the carbon in C1s XPS and oxygen in O1s XPS have several electronic states. Based on the literatures [44–46], for C1s spectra (Figs 6A and 6B), the main peak at 284.6–284.7 eV is attributed to graphitized carbon (C=C). The other three peaks should be attributed to the defects on the GF structure (C—C, 285.1 eV), C—OH (286.0–286.3 eV), C=O (286.8–287.0 eV). Regarding the O1s spectra (Figs 6C and 6D), the split peaks located at 532.2–532.7 eV, 531.0–531.1 eV, 533.9–534.2 eV should be assigned to —OH, C=O, and adsorbed molecular water (H—O—H), respectively.

The relative content of these surface groups of the samples were obtained by measuring the relative peak areas based on Figs 6 and the results are listed in Table 1. It can be seen that the content of

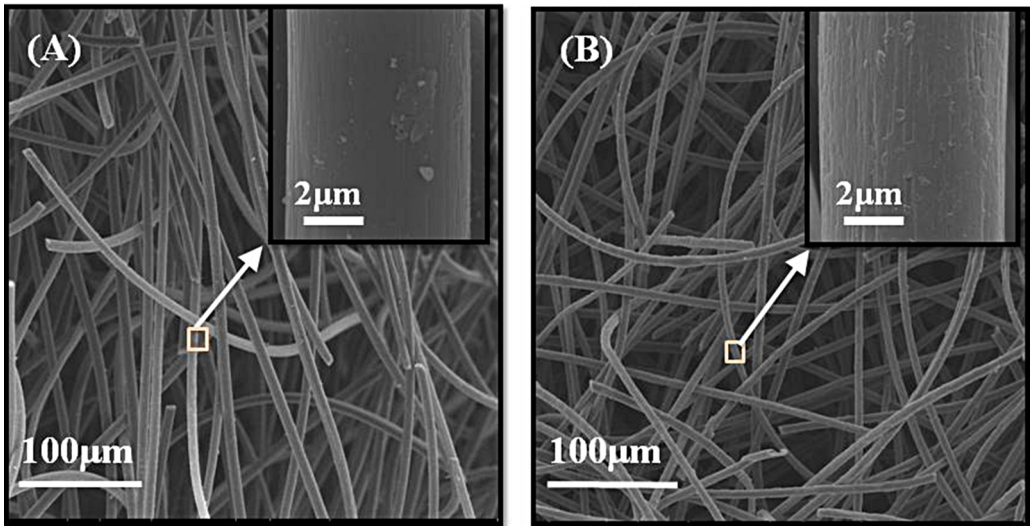

Fig. 4. SEM images of RGF (A) and AGF-900 (B).

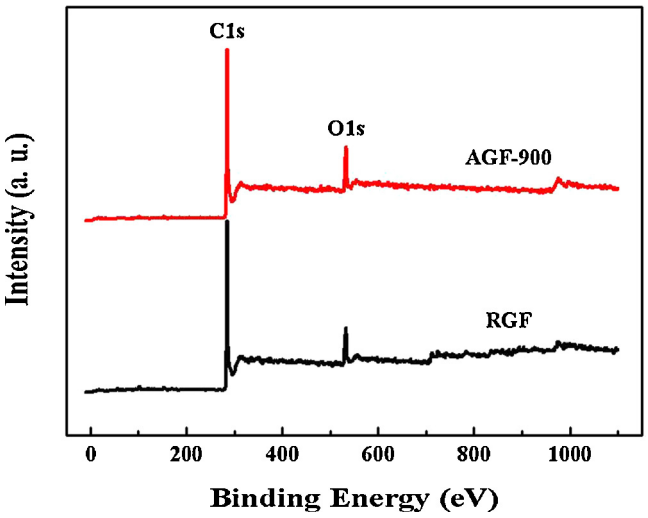

Fig. 5. XPS general spectra of RGF and AGF-900.

—OH and C=O at the surface of GF is increased from 7.16% to 8.26% and from 3.74% to 4.00%, respectively, demonstrating an increase of oxygen-containing functional groups after KOH activation. It is worth noticing that these oxygen-containing groups will provide hydrophilic properties to the GF surface, so it is readily accessible for the dissolved oxygen to diffuse close to the surface, facilitating the ORR to generate H_2O_2 [47]. Moreover, they could be acted as the surface-active sites capable of accelerating the electrochemical reactions [47]. Besides, the content of H—O—H was increased as a result of the improved hydrophilicity of the surface caused by the increase of —OH group [44].

3.3.3. Contact angle

In order to obtain the wettability of GF, the contact angle of water at RGF and AGF-900 surface were measured and are schematically shown in Fig. 7. As it can be seen, the respective initial contact angle of RGF and AGF-900 is 149.10° and 131.40°, confirming the improvement of the wettability of the RGF after KOH activation. This could be resulted from the introduced oxygen-containing functional groups onto the RGF surface through KOH activation. Although both wettability values of RGF and AGF-900 do not change a lot with time, indicating that the surface energy of

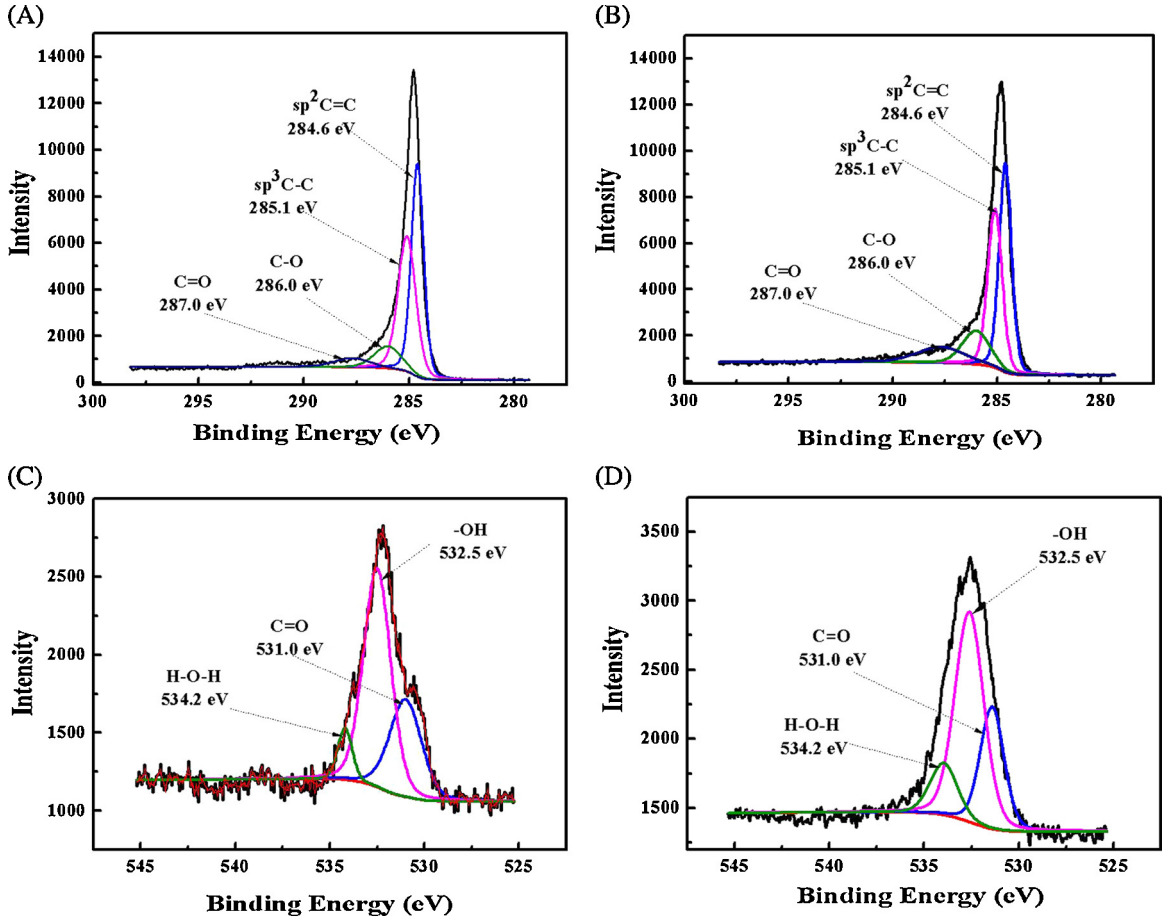

Fig. 6. XPS C1s peaks of RGF (A) and AGF-900 (B), and O1s peaks of RGF (C) and AGF-900 (D).

Table 1
The contents of oxygen-containing groups on the surface of RGF and AGF-900.

Sample	O/C ratio	C=C and C—C (%)	O (%)	Oxygen-containing groups		
				C—OH (%)	C=O (%)	H—O—H (%)
RGF	0.14	84.41	11.81	7.16	3.74	0.90
AGF-900	0.17	84.32	14.21	8.26	4.00	1.95

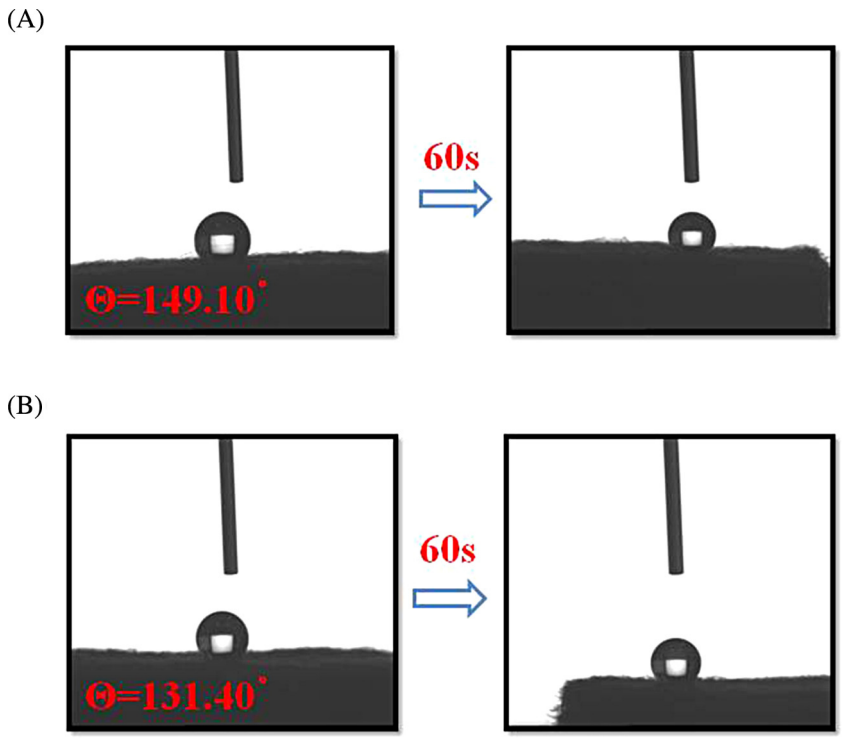

Fig. 7. Contact angle measurements of RGF (A) and AGF-900 (B).

AGF-900 is still very low and the wettability is still poor, it is not to deny that the wettability of the RGF was significantly improved after the treatment [46].

3.4. H_2O_2 accumulation at AGF-900 in the EF system

Considering that H_2O_2 generation rate is a very important parameter for the EF process and the applied cathodic potential is a key determining factor for H_2O_2 generation, the H_2O_2 accumulation at AGF-900 was then investigated at different applied cathode potentials and the results are given in Fig. 8. As one can distinguish, H_2O_2 concentration increases as the cathode potential is increased from −0.3 V to −0.7 V and reaches the maximal value (79.2 mg L^{-1}) at −0.7 V. However, as the cathode potential is further increased, H_2O_2 concentration decreases due to the occurrence of both reduction of H_2O_2 to H_2O and H_2 evolution reaction which is a side reaction and restrains the ORR to generate H_2O_2. These results are in agreement with the LSV results (Fig. 1).

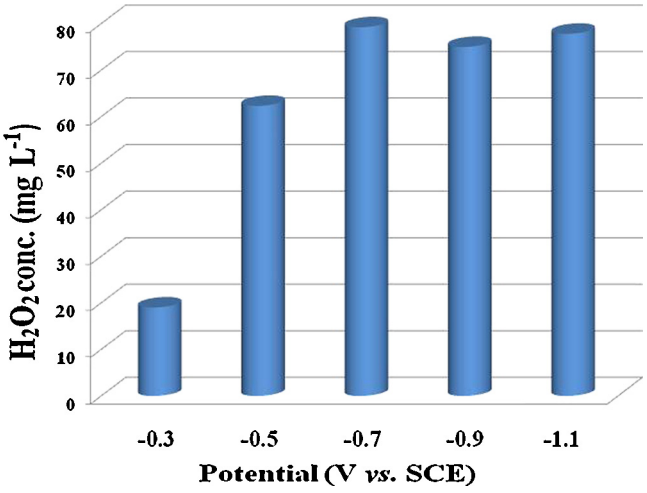

Fig. 8. Accumulation of H_2O_2 at RGF and AGF-900 in 2 h at different applied cathode potentials. The electrolyte was 0.1 mol L^{-1} Na_2SO_4 and the solution pH value was 3.0.

3.5. DMP degradation at AGF-900 in the EF system

3.5.1. Comparison of adsorption, oxidation by oxygen and electrogenerated H_2O_2, and EF process

In the EF process for DMP degradation at AGF-900 cathode, the DMP adsorption by AGF-900 electrode itself and its direct oxidation by O_2 and the oxidation by the electrogenerated H_2O_2 probably contribute to the decrease of the DMP concentration. To investigate the above influence on DMP degradation, additional experiments were carried out and the results are presented in Fig. 9. It can be clearly seen that there is only a slight difference between the DMP removal percentages by pure adsorption, oxidation by O_2 and the oxidation by the electrogenerated H_2O_2. In all the above three cases, only 4–9% of DMP is removed, which means that neither adsorption, oxidation by O_2 nor the oxidation by the electrogenerated H_2O_2 is an effective way for DMP removal. On the contrary, the EF technology has a much higher DMP removal percentage and DMP can be completely removed within 45 min. Therefore, it is not difficult to conclude that the main DMP removal was achieved through the EF process.

3.5.2. Effect of applied cathode potential

In order to obtain the optimal applied cathode potential for DMP degradation, a set of experiments with different applied cathode potentials were carried out and the corresponding results are shown in Fig. 10. DMP degradation rate increases rapidly as the applied cathode potential increases in the potential range from −0.3 V to −0.7 V, whereas from −0.7 V to −1.1 V, the apparent rate constants are close to about 0.19 min^{-1} (Fig. 10A). However, in the case of −0.9 V and −1.1 V, the energy consumption is significantly higher than that at −0.7 V, as displayed in Fig. 10B. Meanwhile,

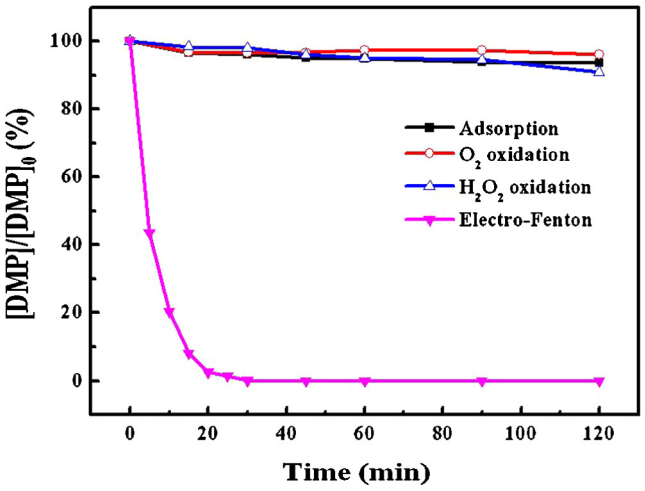

Fig. 9. Variation of DMP removal percentage with time at pH 3.0. For adsorption: no oxygen was supplied and the current was turned off. For oxidation by O_2: oxygen sparging rate was 600 mL min^{-1}. For H_2O_2 oxidation: oxidation with electrogenerated H_2O_2 at −0.7 V without Fe^{2+} addition. For electro-Fenton: applied cathode potential was −0.7 V.

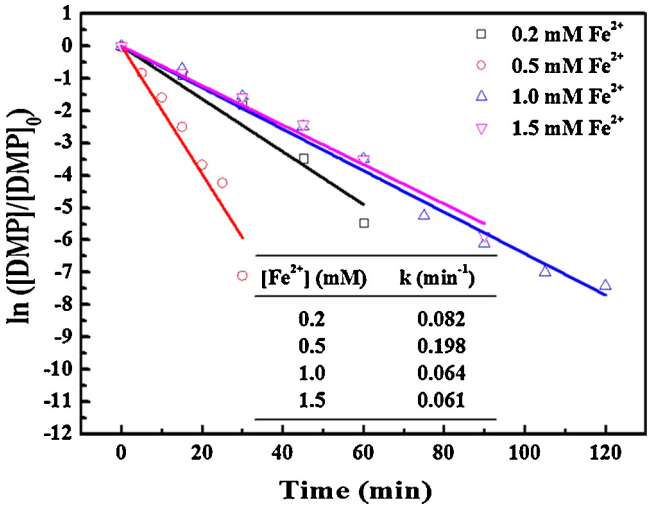

Fig. 11. Effects of initial Fe^{2+} concentration on DMP degradation kinetics at AGF-900, initial DMP concentration: 50.0 mg L^{-1}, initial pH = 3.0, applied cathode potential: −0.7 V.

comparing these results at −0.7 V, −0.5 V and −0.3 V, although the energy consumption is almost the same, the apparent rate constant at −0.7 V is obviously higher. Therefore, the optimal applied cathode potential for DMP degradation at AGF-900 cathode is close to −0.7 V.

3.5.3. Effect of initial Fe^{2+} concentration

Fe^{2+} cations play an important role in initiating the decomposition of H_2O_2 to generate •OH in the Fenton process, according to Eq. (2) [48]. However, higher Fe^{2+} concentrations inhibit the mineralization process by the rapid consumption of •OH radicals through the following reaction (Eq. (6)) [49–51].

$$Fe^{2+} + {}^{\bullet}OH \rightarrow Fe^{3+} + OH^{-} \quad (6)$$

Therefore, Fe^{2+} concentration should be properly controlled. In order to investigate the effect of initial Fe^{2+} concentration on DMP degradation performance, a set of experiments with different initial Fe^{2+} concentration values were carried out. As seen from Fig. 11, the apparent rate constant of DMP degradation increases from 0.082 min^{-1} to 0.198 min^{-1} as the initial Fe^{2+} concentration increases from 0.2 mmol L^{-1} to 0.5 mmol L^{-1}. This could be due to the increased amount of generated •OH radicals through Eq. (2). However, the apparent rate constant of DMP degradation decreases to 0.061 min^{-1} as the initial Fe^{2+} concentration further increases to 1.5 mmol L^{-1}, probably resulting from the reaction between Fe^{2+} and •OH (Eq. (6)). This reaction is several orders of magnitude faster than the •OH generation reaction. Therefore, it can be concluded that the optimal initial Fe^{2+} concentration is 0.5 mmol L^{-1}.

3.5.4. Recycling performance

The recycling performance of AGF-900 cathode for DMP degradation was investigated. As clearly presented in Fig. 12, there is no significant decay after AGF-900 electrode was reused for DMP degradation at −0.7 V for 20 times. Moreover, DMP can be almost completely and quickly degraded within 1 h, indicating that AGF-900 electrode is a promising EF cathode because of its excellent recycling performance, such as good stability, repeatability and desirable DMP degradation performance.

3.5.5. Comparison with other cathode materials for DMP degradation performance

In order to further check the effectiveness of AGF-900 as EF cathode, the other commonly used EF cathodes (with the same geometric area) were used for DMP degradation. As shown in Fig. 13, AGF-900 has a distinct superiority, with the complete DMP

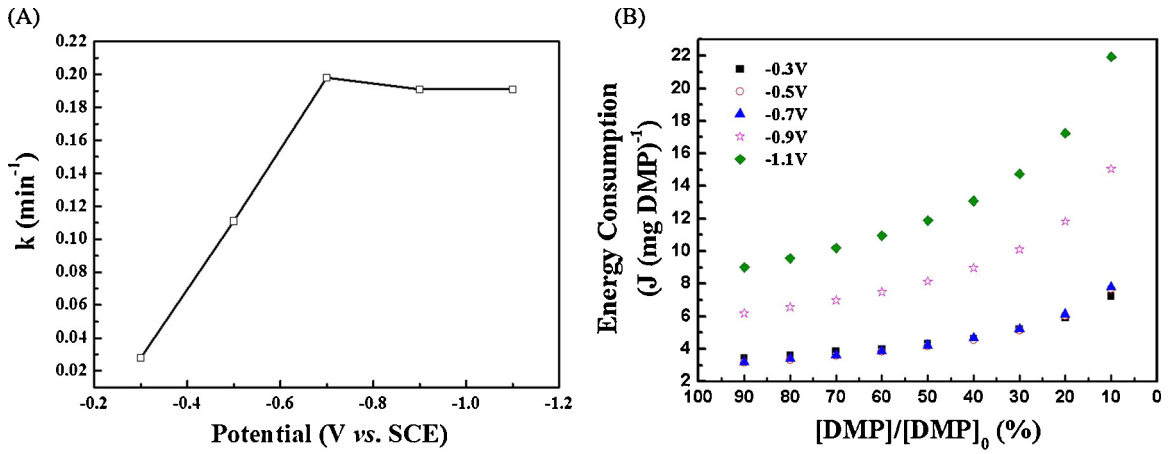

Fig. 10. Effects of applied cathodes potential on the DMP degradation kinetics (A) and energy consumption (B) at AGF-900, initial DMP concentration: 50.0 mg L^{-1}, initial pH = 3.0, [Fe^{2+}] = 0.5 mmol L^{-1}.

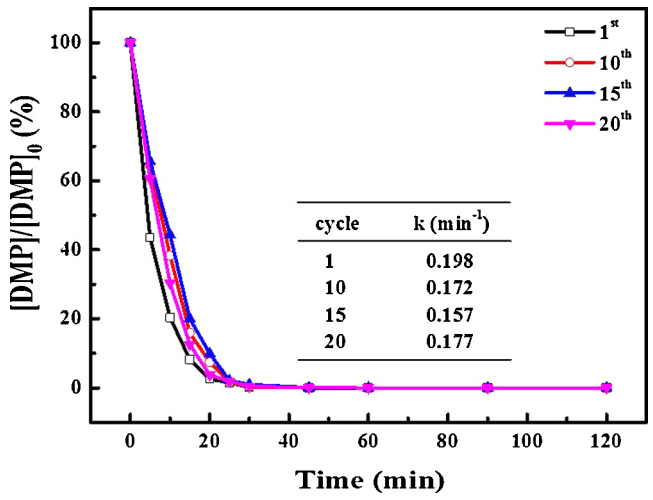

Fig. 12. The recycling experiments of AGF-900 for DMP degradation, initial DMP concentration: 50 mg L^{-1}, initial pH = 3.0, $[Fe^{2+}]$ = 0.5 mmol L^{-1}, applied cathode potential: −0.7 V.

degradation within 45 min, with respect to about 30.5%, 37.1% 39.7%, and 87.3% degradation of the initial DMP concentration at MWCNT *gas diffusion electrode* (GDE), XC-72R carbon black GDE, graphite GDE (the detailed preparation information was described in the supplementary materials), and *carbon nanotube sponge* (CNTS), respectively. Their corresponding apparent rate constants for DMP degradation are 0.007, 0.009, 0.011, 0.057 and 0.198 min^{-1} at MWCNT GDE, XC-72R carbon black GDE, graphite GDE, CNTS and AGF-900, respectively. Obviously, AGF-900 exhibits the most desirable DMP degradation efficiency among all the present investigated EF cathodes, demonstrating again that the AGF-900 electrode is a promising EF cathode in wastewater treatment.

3.6. Degradation of other contaminants at AGF-900 EF cathode

In order to investigate the universality of AGF-900 electrode, it was adopted to degrade some other contaminants in the wastewater, such as *diethyl phthalate* (DEP), *dibutyl phthalate* (DBP), *nitrobenzene* (NB), aniline, and *rhodamineB* (RhB). Their degradation percentage and the corresponding apparent rate constant (k) (pseudo first-order reaction) are given in Fig. 14. The comparative results can be further clearly seen from the summarized results listed in Table 2. As seen, all the present investigated contaminants can be completely degraded within 2 h. Compared with the reported results [52–56], AGF possesses much better performance in terms of either higher *k* value for degrading organic contaminants, degradation percentage or *total organic carbon* (TOC) removal. This indicates that AGF-900 can be employed universally as the cathode in EF system for removing organic contaminants.

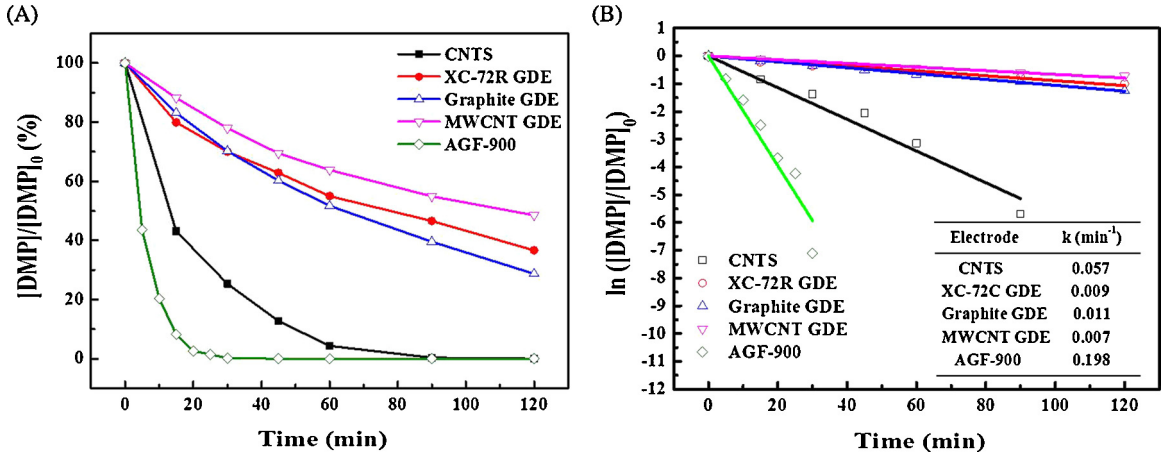

Fig. 13. Comparison with other cathodes for DMP degradation efficiency (A) and kinetics (B), initial DMP concentration: 50.0 mg L^{-1}, initial pH = 3.0, $[Fe^{2+}]$ = 0.5 $mmol^{-1}$, applied cathode potential: −0.7 V.

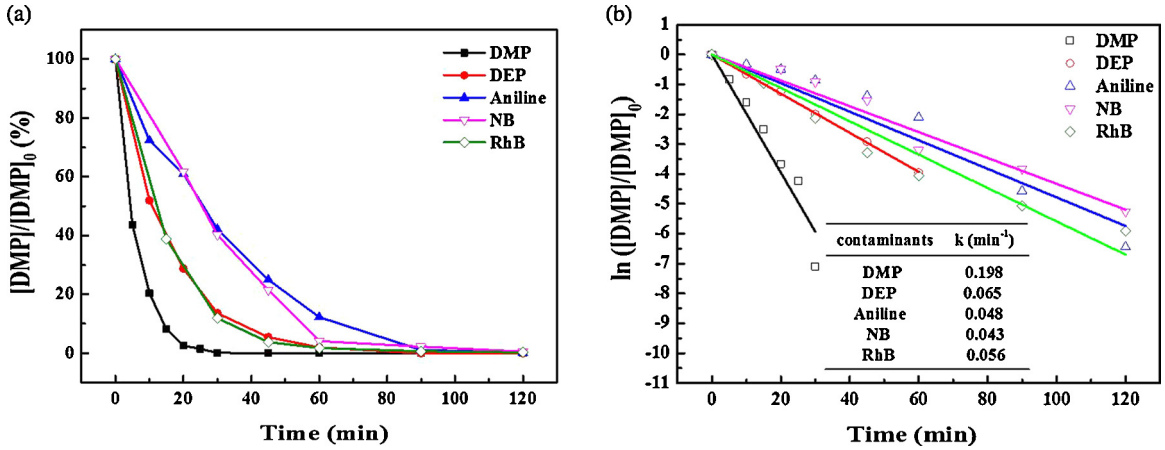

Fig. 14. Degradation efficiency (A) and kinetics (B) of various contaminants at AGF-900 cathode, initial contaminant concentration: 50.0 mg L^{-1}, initial pH = 3.0, $[Fe^{2+}]$ = 0.5 mmol L^{-1}, applied cathode potential: −0.7 V.

Table 2
Degradation of various contaminants at AGF-900 cathode and comparison with the reported results.

No.	Contaminants	Initial conc. (ppm)	Time (min)	Degradation (%)	TOC elimination (%)	k (min^{-1})	The reported results	Ref.
1	DMP	50	45	100	100	0.198	k = 0.00069–0.0028 min^{-1} (EF-like)	[45]
2	DEP	50	90	100	80	0.065	80.9% DEP was removed after 9 h.	[46]
3	NB	50	120	100	65	0.043	49% TOC was removed after 3 h.	[47]
4	Aniline	50	120	100	75	0.048	68% TOC was removed after 6 h.	[48]
5	RhB	50	120	100	68	0.056	k = 0.0208 min^{-1}	[49]

4. Conclusions

Graphite felt was successfully decorated with high surface area and functionalized with oxygen-containing groups through KOH activation at high temperature. This favors H_2O_2 generation through oxygen reduction reaction, and thus accelerating the DMP degradation with activated graphite felt as the EF cathode.

With the optimized KOH activation process, i.e. at 900 °C for 1 h, AGF-900 exhibited the highest DMP degradation performance at −0.7 V at the optimized Fe^{2+} concentration of 0.5 mmol L^{-1} with an apparent rate constant of 0.198 min^{-1}, about 10 times that at raw graphite felt (0.020 min^{-1}) and desirable stability without significant performance decay after 20 times recycling for DMP degradation reaction with a reaction time of 2 h each. Moreover, AGF-900 could also degrade efficiently the other organic contaminants.

Last but not the least, AGF-900 can be employed universally to remove a variety of contaminants, which makes it an attractive alternative cathode for EF system to deal with wastewaters.

Acknowledgements

This work was supported by the Natural Science Foundation of China (21107145, 21077136), the project of Pearl River Science and Technology New Star of Guangzhou (2011Z220061), the Fundamental Research Funds for the Central Universities of China (12lgpy13). We also thank the Fund for Fostering Talents in National Basic Science for funding. Prof. Tsiakaras is grateful for funding to the research program "Bilateral R&D Co-operation between Greece-China 2012-2014", which is co-financed by the European Union and the Greek Ministry of Education-GSRT.

Appendix A. Supplementary data

Supplementary material related to this article can be found, in the online version, at http://dx.doi.org/10.1016/j.apcatb.2014.09.074.

References

[1] A. Thiam, M. Zhou, E. Brillas, I. Sirés, Appl. Catal. B: Environ. 150–151 (2014) 116–125.
[2] R. Thiruvenkatachari, T.O. Kwon, J.C. Jun, S. Balaji, M. Matheswaran, I.S. Moon, J. Hazard. Mater. 142 (2007) 308–314.
[3] N. Merayo, D. Hermosilla, L. Blanco, L. Cortijo, A. Blanco, J. Hazard. Mater. 262 (2013) 420–427.
[4] R.M. Mohamed, E. Aazam, Chin. J. Catal. 34 (2013) 1267–1273.
[5] S.L. Zhang, X.M. Hu, X.W. Wang, S.J. Liang, L. Wu, Chin. J. Catal. 33 (2012) 1736–1741.
[6] M. Antonopoulou, E. Evgenidou, D. Lambropoulou, I. Konstantinou, Water Res. 53 (2014) 215–234.
[7] M.A. Oturan, J.J. Aaron, Crit. Rev. Environ. Sci. Technol. 44 (2014) 2577–2641.
[8] E. Rosales, M. Pazos, M.A. Sanromán, Chem. Eng. Technol. 35 (2012) 609–617.
[9] Z. Ai, T. Mei, J. Liu, J. Li, F. Jia, L. Zhang, J. Qiu, J. Phys. Chem. C 111 (2007) 14799–14803.
[10] Y. Wang, G. Zhao, S. Chai, H. Zhao, Y. Wang, ACS Appl. Mater. Interfaces 5 (2013) 842–852.
[11] E. Brillas, I. Sirés, M.A. Oturan, Chem. Rev. 109 (2009) 6570–6631.
[12] X.H. Yan, G.R. Zhang, B.Q. Xu, Chin. J. Catal. 34 (2013) 1992–1997.
[13] Z.W. Wang, B. Li, Y.C. Xin, J.G. Liu, Y.F. Yao, Z.G. Zou, Chin. J. Catal. 35 (2014) 509–513.
[14] A. Brouzgou, S.Q. Song, P. Tsiakras, Appl. Catal. B: Environ. 127 (2012) 371–388.
[15] S. Yuan, Y. Fan, Y. Zhang, M. Tong, P. Liao, Environ. Sci. Technol. 45 (2011) 8514–8520.
[16] C.T. Wang, J.L. Hu, W.L. Chou, Y.M. Kuo, J. Hazard. Mater. 152 (2008) 601–606.
[17] M. Pimentel, N. Oturan, M. Dezotti, M.A. Oturan, Appl. Catal. B: Environ. 83 (2008) 140–149.
[18] S. Hammami, N. Oturan, N. Bellakhal, M. Dachraoui, M.A. Oturan, J. Electroanal. Chem. 610 (2007) 75–84.
[19] N. Oturan, M. Zhou, M.A. Oturan, J. Phys. Chem. A 114 (2010) 10605–10611.
[20] M. Panizza, M.A. Oturan, Electrochim. Acta 56 (2011) 7084–7087.
[21] M. Zhou, Q. Tan, Q. Wang, Y. Jiao, N. Oturan, M.A. Oturan, J. Hazard. Mater. 215–216 (2012) 287–293.
[22] M. Panizza, G. Cerisola, Water Res. 35 (2001) 3987–3992.
[23] A. Özcan, Y. Şahin, A. Savaş Koparal, M.A. Oturan, J. Electroanal. Chem. 616 (2008) 71–78.
[24] A. Wang, J. Qu, J. Ru, H. Liu, J. Ge, Dyes Pigments 65 (2005) 227–233.
[25] C.T. Wang, W.L. Chou, M.H. Chung, Y.M. Kuo, Desalination 253 (2010) 129–134.
[26] H. Lei, H. Li, Z. Li, Z. Li, K. Chen, X. Zhang, H. Wang, Process Saf. Environ. Prot. 88 (2010) 431–438.
[27] Y. Sheng, S. Song, X. Wang, L. Song, C. Wang, H. Sun, X. Niu, Electrochim. Acta 56 (2011) 8651–8656.
[28] H. Wang, J. Wang, Appl. Catal. B: Environ. 77 (2007) 58–65.
[29] N. Borràs, C. Arias, R. Oliver, E. Brillas, Chemosphere 85 (2011) 1167–1175.
[30] F.C. Moreira, S. Garcia-Segura, R.A.R. Boaventura, E. Brillas, V.J.P. Vilar, Appl. Catal. B: Environ. 160–161 (2014) 492–505.
[31] E. Isarain-Chávez, C. Arias, P.L. Cabot, F. Centellas, R.M. Rodríguez, J.A. Garrido, E. Brillas, Appl. Catal. B: Environ. 96 (2010) 361–369.
[32] M. Zarei, A. Niaei, D. Salari, A. Khataee, J. Hazard. Mater. 173 (2010) 544–551.
[33] M. Zarei, D. Salari, A. Niaei, A. Khataee, Electrochim. Acta 54 (2009) 6651–6660.
[34] L. Zhou, Z. Hu, C. Zhang, Z. Bi, T. Jin, M. Zhou, Sep. Purif. Technol. 111 (2013) 131–136.
[35] L. Zhou, M. Zhou, C. Zhang, Y. Jiang, Z. Bi, J. Yang, Chem. Eng. J. 233 (2013) 185–192.
[36] J.J. Niu, J.N. Wang, Y. Jiang, L.F. Su, J. Ma, Micropor. Mesopor. Mater. 100 (2007) 1–5.
[37] C. He, S. Song, J. Liu, V. Maragou, P. Tsiakaras, J. Power Sources 195 (2010) 7409–7414.
[38] H. Liu, C. Wang, X. Li, X. Xuan, C. Jiang, H. Cui, Environ. Sci. Technol. 41 (2007) 2937–2942.
[39] B.L. Yuan, X.Z. Li, N. Graham, Water Res. 42 (2008) 1413–1420.
[40] B.L. Yuan, X.Z. Li, N. Graham, Chemosphere 72 (2008) 197–204.
[41] Y. Chen, Z. Ai, L. Zhang, J. Hazard. Mater. 235–236 (2012) 92–100.
[42] J.B. Wang, C. Wang, C.L. Yang, G.Q. Wang, W.P. Zhu, Chin. J. Catal. 34 (2013) 313–321.
[43] Y. Wang, Y. Liu, T. Liu, S. Song, X. Gui, H. Liu, P. Tsiakaras, Appl. Catal. B: Environ. 156–157 (2014) 1–7.
[44] C. Gao, N. Wang, S. Peng, S. Liu, Y. Lei, X. Liang, S. Zeng, H. Zi, Electrochim. Acta 88 (2013) 193–202.
[45] L. Yue, W.S. Li, F.Q. Sun, L.Z. Zhao, L.D. Xing, Carbon 48 (2010) 3079–3090.
[46] W. Zhang, J. Xi, Z. Li, H. Zhou, L. Liu, Z. Wu, X. Qiu, Electrochim. Acta 89 (2013) 429–435.
[47] J. Miao, H. Zhu, Y. Tang, Y. Chen, P. Wan, Chem. Eng. J. 250 (2014) 312–318.
[48] W. Cheng, M. Yang, Y. Xie, B. Liang, Z. Fang, E.P. Tsang, Chem. Eng. J. 220 (2013) 214–220.
[49] E. Guinea, J.A. Garrido, R.M. Rodríguez, P.L. Cabot, C. Arias, F. Centellas, E. Brillas, Electrochim. Acta 55 (2010) 2101–2115.
[50] N. Masomboon, C. Ratanatamskul, M.C. Lu, J. Hazard. Mater. 176 (2010) 92–98.
[51] G. Zhang, F. Yang, M. Gao, X. Fang, L. Liu, Electrochim. Acta 53 (2008) 5155–5161.
[52] C.T. Wang, Y.J. Hua, Y.X. Tong, Electrochim. Acta 55 (2010) 6755–6760.
[53] H. Wang, D.Z. Sun, Z.Y. Bian, J. Hazard. Mater. 180 (2010) 710–715.
[54] E. Brillas, M.A. Baños, S. Camps, C. Arias, P.L. Cabot, J.A. Garrido, R.M. Rodríguez, New J. Chem. 28 (2004) 314–322.
[55] E. Brillas, E. Mur, R. Sauleda, L. Sànchez, J. Peral, X. Domènech, J. Casado, Appl. Catal. B: Environ. 16 (1998) 31–42.
[56] P.V. Nidheesh, R. Gandhimathi, N.S. Sanjini, Sep. Purif. Technol. 132 (2014) 568–576.